MELT-ROCK INTERACTION BETWEEN GRANITIC PEGMATITES AND HOSTING AMPHIBOLITES FROM THE CHIAVENNA OPHIOLITIC UNIT (TANNO PEGMATITIC FIELD, CENTRAL ALPS, NORTH ITALY)

Francesco Arrigoni*, **Patrizia Fumagalli***,✉, **Stefano Zanchetta**** and **Alessandro Guastoni*****

* *Dipartimento di Scienze della Terra "Ardito Desio", Università degli Studi di Milano, Italy.*
** *Dipartimento di Scienze dell'Ambiente e della Terra, Università degli Studi di Milano Bicocca, Italy.*
*** *Dipartimento di Geoscienze, Università di Padova, Italy.*
✉ *Corresponding author, email: patrizia.fumagalli@unimi.it*

Keywords: *Melt-rock interaction; pegmatites; amphibolites; Chiavenna Ophiolitic Unit; Central Alps.*

ABSTRACT

The Tanno pegmatitic field, placed southward of Chiavenna (Central Alps, Sondrio, Italy), develops a large number of subplanar dykes that crosscut the Chiavenna Unit, an ophiolitic complex mainly composed, in the study area, of amphibolite rocks. This study focuses on the contact between a pegmatitic dyke and the amphibolitic country rock. We distinguished four zones across the contact: I) inner amphibolite, II) contact amphibolite, III) contact pegmatite, IV) inner pegmatite. The inner amphibolite, not affected by melt-rock interaction, is composed of amphibole, phlogopite, ilmenite, titanite and rutile. Two amphibole generations occur, both of them showing a patchy compositional zoning. Amphibole I are Mg-hornblende, whereas Amphibole II have a pargasitic composition. The contact amphibolite shows an enrichment of mica belonging to the phlogopite-biotite series, titanite and the presence of fluorapatite and plagioclase (Ab_{45-60}), that is absent in the inner amphibolite. Close to the contact, amphiboles display no zoning and gain an Mg-horneblenditic composition. The contact pegmatite has quartz, albitic plagioclase, garnet (almandine-spessartine series), muscovite, K-feldspar and fluorapatite. It shows a comb texture, with elongation of plagioclase crystals normal to the contact itself. Far from the contact, the inner pegmatite has an increasing grain-size and a less organized texture. In this zone several accessory phases occur, including gahnite, columbite-(Fe), monazite-(Ce), xenotime-(Y), uraninite and betafite. Whole rock analyses suggest that a chemical exchange, concerning both major elements and trace elements, occurred between the pegmatitic melt and the hosting amphibolite. A considerable increase of SiO_2, Na_2O and, to a lesser extent, of Al_2O_3 is observed from the amphibolite towards the pegmatite; K_2O and CaO show a decrease at the same extent. The REE pattern in the pegmatite highlights an enrichment in HREE at the contact. Mineral chemistry confirms this trend with variations observable in plagioclase, gradually more albitic from the amphibolite to the pegmatite. Mineralogical characters and geochemical features allow to classify the Tanno pegmatite in the LCT (Lithium, Cesium, Tantalium) family. Based on the metamorphic peak conditions reported from the Lepontine Dome the ambient conditions during pegmatite intrusion were ca. 550°C and 5 kbar. The reduced thermal difference between pegmatite and wall rock explains the diffuse contact observed by X-ray micro-computed tomography. The collected data suggest a chemical interaction between melt and wall rock, according to the following reaction taking place in the amphibolite

Amphibole I + Amphibole II + Ilmenite + Pegmatitic melt → Amphibole III + Plagioclase + Phlogopite + Titanite + Fluorapatite

INTRODUCTION

The development of a pegmatite field in the Valchiavenna area is related to the emplacement of the Novate Granite, which occurred about 24±1.2 Ma (zircon U-Pb ages; Liati et al., 2000). The northernmost field is located south of Chiavenna and close to the Tanno village (Fig. 1), where pegmatites intruded the Chiavenna Unit, an ophiolitic complex consisting mainly of serpentinites, amphibolites and minor metagabbros.

The intrusion of the Tanno pegmatite and aplitic dykes into the amphibolites of the Chiavenna Unit has led to metasomatic reactions and the development of geochemical gradients. Although several studies deal with the Tanno pegmatitic field, they mainly focus on minerals of gemmological and collecting interest, while poor attention has been given to the metasomatic reactions involving the country rocks.

The aim of this study is to investigate the relationships between dykes and the wall rocks, on the basis of main mineralogical changes and the temperature-pressure regime at the time of the pegmatitic melt emplacement.

GEOLOGICAL SETTING

The area of interest is located in Valchiavenna (Val Mera, Central Alps, N Italy), which extends N-S from the northern tip of Lake Como (Fig. 1). The central Alps section of the Alpine belt is characterized by Barrovian-type metamorphism of Cenozoic age with high-grade metamorphic rocks exposed in the so called "Lepontine Dome" (Trommsdorf, 1966) with roughly concentric metamorphic isogrades. The Barrovian overprint is abruptly truncated to the south by the Insubric Fault, a major structure, active since the Oligocene (Schmid et al., 1989), that divides the north Alps belt from the south-vergent Southalpine domain. In the Valchiavenna area, North of the Insubric Fault, the Alpine nappe stack consists chiefly of: (i) Penninic units derived from distal European margin (Adula Nappe); (ii) the Chiavenna and Misox Zone ophiolites derived from the Valais Ocean (Steinmann and Stille, 1999; Stucki et al., 2003); (iii) the Tambò and Suretta units, derived from the Brianconnais microcontinent (Schmid et al., 1990); (iv) the Gruf Complex, a metamorphic complex with HT-LP metamorphism, of debated age (Galli et al., 2012; Nicollet et al., 2018); (v) thin slivers belonging to the Austroalpine domain along the Insubric Fault; (vi) the Bergell pluton, a composite magmatic unit that intruded the Alpine nappe stack between 33 and 30 Ma (Von Blanckenburg, 1992; Rosenberg et al., 1995).

The southern part of the Lepontine Dome is characterized by the widespread occurrence of migmatites, pegmatites and leucogranites (e.g. Guastoni et al., 2014). Such occurrences are due to crustal anatexis limited to the area close to the

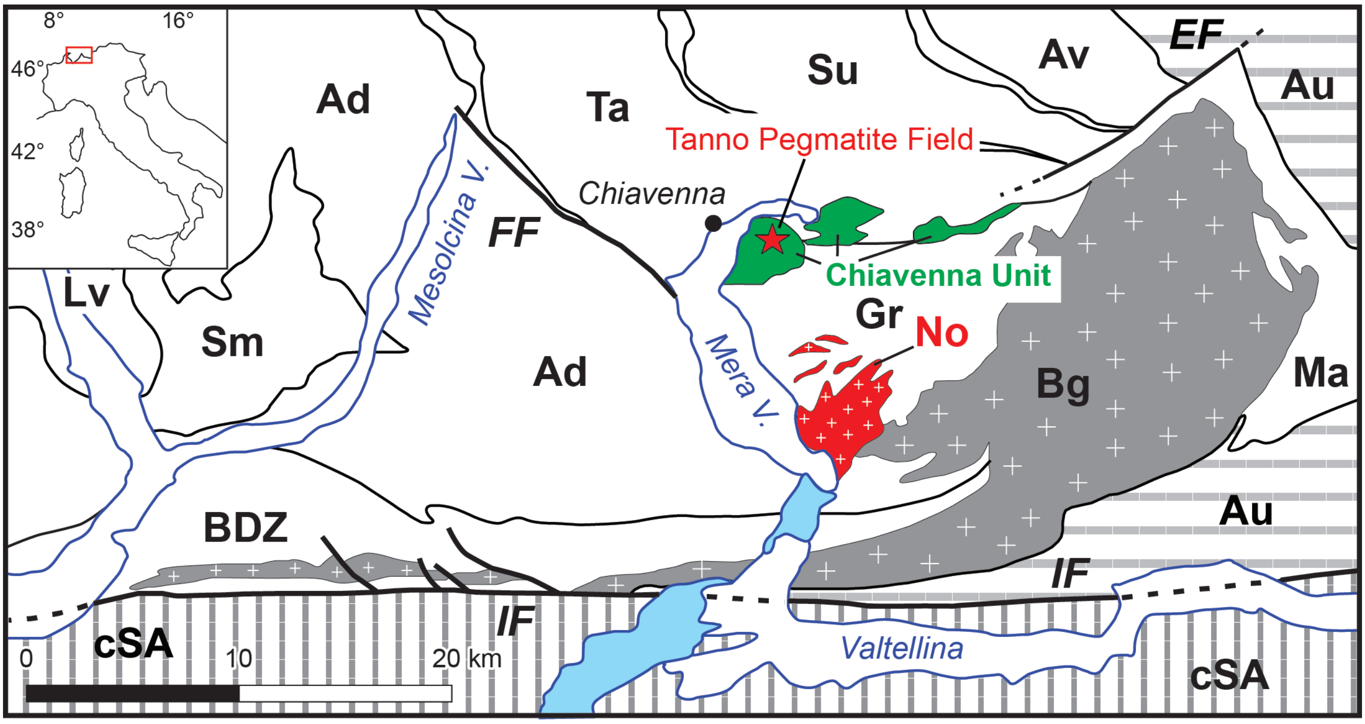

Fig. 1 - Simplified tectonic scheme of the Central Alps. The location of the Tanno pegmatite field is marked with a red star. Ad- Adula nappe; Av- Avers bundnerschiefers; Au- Austroalpine units; BDZ- Bellinzona-Dascio Zone; Bg- Bergell pluton; cSA- central Southern Alps; G-: Gruf complex; Ma- Malneco unit; Lv- Leventina nappe; No- Novate granite; Sm- Simano nappe; Su- Suretta nappe; Ta- Tambò nappe. EF- Engadine Fault; FF- Forcola Fault; IF- Insubric Fault.

Insubric Fault (Burri et al., 2005) and are related to protracted fluid-induced melting that took place in the 32 Ma to 22 Ma time lapse (Rubatto et al., 2009). The most prominent feature of this event in the Chiavenna area is the Novate granite body (Fig.1), a two-mica leucogranite which intrusion is constrained at 24±1.2 Ma (Liati et al., 2000). The northern boundaries of the southern migmatite belt (Burri et al., 2005) runs in the Valchiavenna area just N of Chiavenna along the Italian Bregaglia Valley (Fig. 1), with ophiolites of the Chiavenna Unit that are located within the area where migmatisation occurred.

The Chiavenna Unit represents an incomplete ophiolitic complex, in which subcontinental mantle rocks, instead of oceanic lithosphere, have been tectonically exposed on the ocean floor and covered by N-MORB basalts (Liati et al., 2003). The age of the ophiolites has been constrained to the Late Jurassic - 93±0.2 Ma (Liati et al., 2003) - representing the youngest remnants of the Valais ocean exposed in the Central Alps. The entire unit experienced an amphibolites facies syntectonic metamorphism (Ring, 1992).

The Chiavenna Unit crops out in three areas, alternated with metacarbonates, located on the left side of Chiavenna and Bregaglia valleys, between Aurosina Valley to the North and Prata Camportaccio village to the S.

The ultramafic rocks consist mainly of lherzolites deformed and serpentinized during the Alpine metamorphism (Huber and Marquer, 1998; Talerico, 2001). Beside ultramafic rocks, lenses of metagabbros occur, usually displaying well-preserved pre-deformation magmatic structure. Regarding the basalt-derived amphibolites, they form more than 50% of the Chiavenna Unit. In the present-day tectonic setting derived from the Alpine deformation, the amphibolites are situated structurally below the metaperidotites. The unit also comprises metacarbonate lenses and layers interleaved with the amphibolites.

The Tanno pegmatite-aplite field, as other similar fields in the Valchiavenna area, is likely genetically related to the Novate leucogranite (Fig. 1). The Novate granite is a S-type two-mica peraluminous leucogranite derived from partial melting of a metapelitic source (Oschidari and Zieger, 1992; von Blanckenburg et al., 1992) and genetically not related to the nearby calc-alkaline Bergell pluton (Fig. 1). The Tanno pegmatitic field exhibits a high degree of differentiation, as demonstrated by the occurrence of some accessory minerals as beryl, columbite, gahnite, uraninite and xenotime. Referring to the Černý and Ercit (2005) classification of granitic pegmatites, these pegmatites belongs to the *rare elements* class, which corresponds to the most differentiated one. Alongside, these pegmatites belong to the LCT (Lithium, Cesium, Tantalum) petrogenetic family of typical peraluminous composition (Černý and Ercit, 2005).

FIELD RELATIONSHIPS BETWEEN PEGMATITIC DYKES AND AMPHIBOLITIC WALL ROCK

The main outcrop of the Tanno pegmatitic field (46°18'52''N, 9°24'19''E) is visible looking southeastward from the town of Chiavenna (Fig. 1). It is a steep vertical cliff composed of mafic and ultramafic rocks crosscut by subplanar set of aplite-pegmatite dykes. These dykes intrude the wall rock on an exposed portion of the left side of Valchiavenna, near the small village of Tanno (Fig. 1). The main outcrop cliff, exposed northward, is made of amphibolites of the Chiavenna Unit, with a vertical extension of more than 100 meters (Fig. 2a). The thickness of dykes ranges from few centimeters to few meters. Pegmatites crosscut amphibolite schistosity and compositional layering.

The thicker dykes are subhorizontal to each other, while

Fig. 2 - a) Aerial view of the Tanno pegmatitic field. Pegmatites cross cut the amphibolites belonging to the Chiavenna Unit. b) Detailed image showing the sampled area, characterized by the contact zone between a pegmatitic dyke and the amphibolitic wall rock.

thinner ones crosscut the ones above, implying an intersection relationship between these two different sets. The thicker dykes have a strike of 265-250° N with a dip angle of 15-20° either toward N or S, while the thinners have a similar strike, but, due to their steeper attitude, they crosscut the thicker ones.

The rock-forming minerals in pegmatites are quartz, K-feldspar, plagioclase, muscovite and garnet whereas beryl, columbite, gahnite, uraninite and xenotime occur as main accessory phases.

Most of the dykes are affected by metasomatic and alteration processes due to late stage fluids circulation along rigid fractures that promoted kaolinization and zeolitization.

Furthermore, at the outcrop scale, the contacts between pegmatite and hosting amphibolite are not sharp (Fig. 2b) and the occurrence of a reaction rim is quite evident, as testified by centimetric aplitic veins that depart from the pegmatite dyke and inject the amphibolite wall rock.

A representative contact between a pegmatitic dike and the host amphibolites was sampled (sample volume 30x20x10 cm^3, Fig. 3) in order to study the melt-rock interactions that occurred during dikes intrusion.

ANALYTICAL METHODS

Major and trace elements whole rock analyses were obtained by inductively-coupled plasma mass spectrometry at Bureau Veritas Mineral Laboratories, Krakow (Poland). Analyzed samples close to the contact were obtained by micro-drilling across the interface between pegmatite and amphibolite. Chemical compositions of mineral phases were obtained with a JEOL JXA-8200 WDS electron microprobe (EPMA) at the Dipartimento di Scienze della Terra "Ardito Desio", University of Milano. Analyses were acquired with an accelerated voltage of 15 kV and a beam current of 15 nA. Typical acquisition time was 30 s counting on peaks and 10 s counting on the background. The standards applied for the different elements are: omphacite (Na), sanbornite (Ba), rodonite (Mn, Zn), K-feldspar (K), olivine (Mg), grossular (Si, Ca, Al), ilmenite (Ti), fayalite (Fe), hornblende (F), graftonite (P), UO_2 (U), pure Cr, pure Nb and pure Ta. Several analyses presented in Supplementary Table 1S, mainly amphiboles and micas, are non-stoichiometric due to the occurrence of elements (e.g. Rb, Sr, U, and F) that were not always measured during the standard EPMA analytical routine or were intrinsically not accurate due to interference problems with other measured elements.

X-ray micro-computed tomography allowed the detailed study of the geometric relationship at the contact between dykes and wall rock. The scans were acquired with a MicroCT/DR BIR Actis 130/150 system, with a resolution of 14 μm at the Dipartimento di Scienze della Terra e

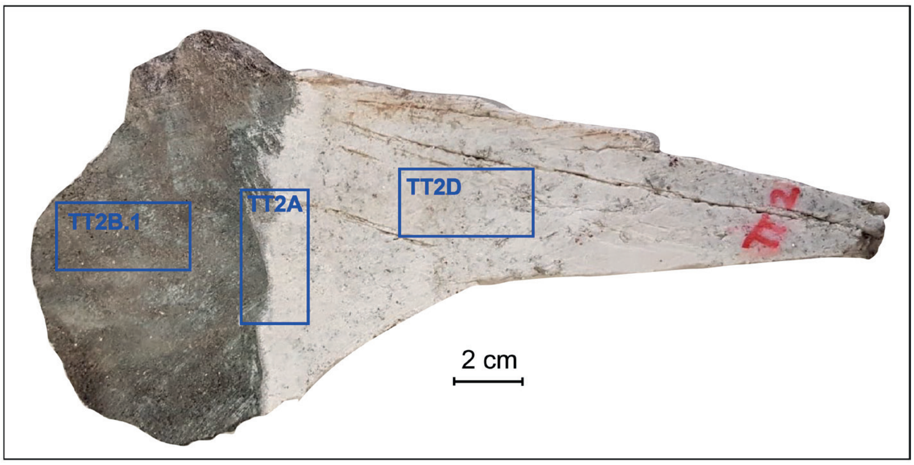

Fig. 3 - Sample TT2 showing the contact between amphibolites and granitic pegmatites from which thin sections TT2B.1 (inner amphibolite), TT2A (amphibolite-pegmatite contact) and TT2D (inner pegmatite) were obtained (indicated by the red rectangles). Other analyzsed samples were collected in the proximity of TT2 along the pegmatite-amphibolite contact.

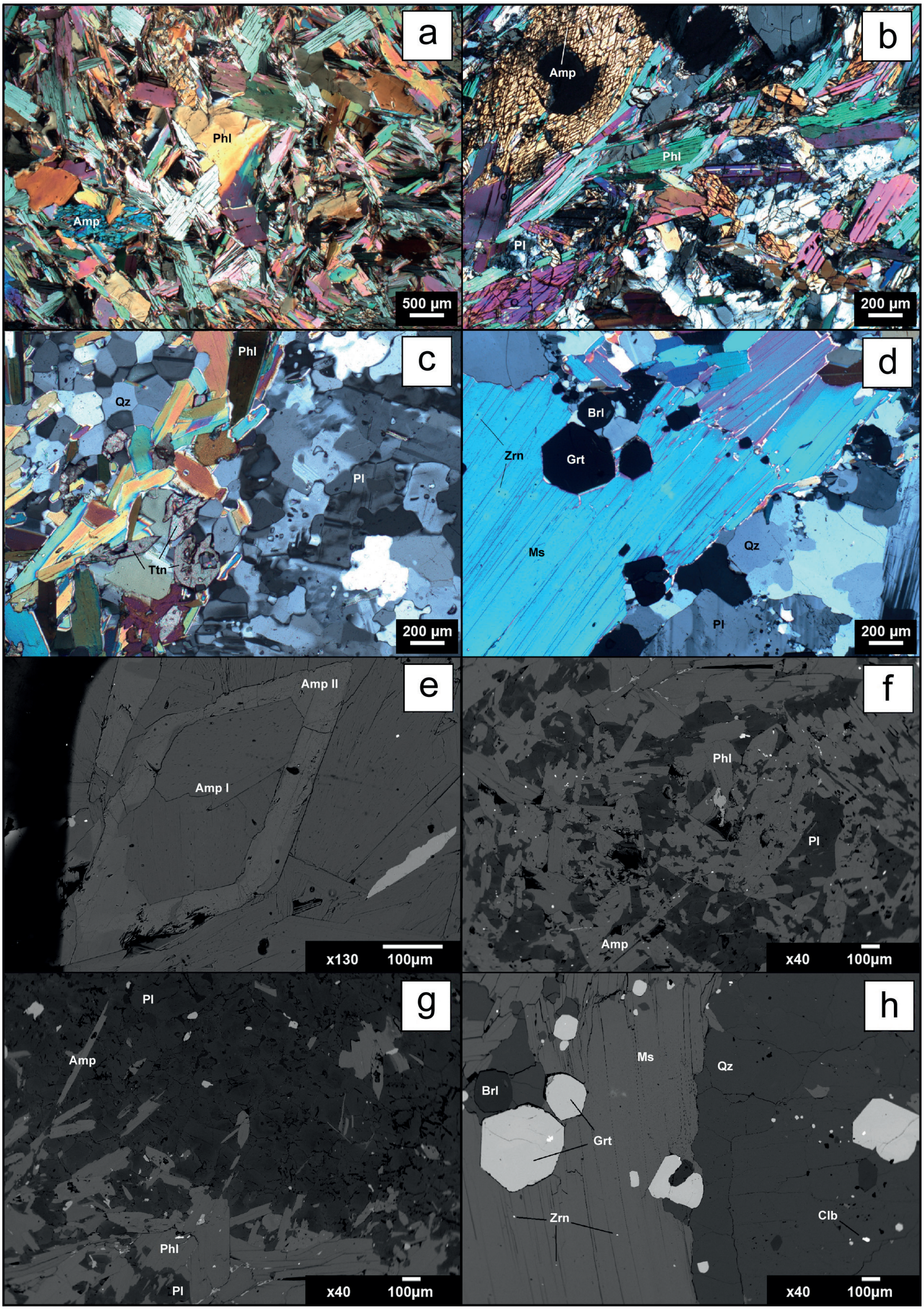

Fig. 4 - Photomicrographs and back-scattered electron images of representative amphibolites and pegmatite samples. a) Mineralogical association of the inner wall rock amphibolites, characterized by the occurrence of amphibole and phlogopite. b) Plagioclase appearance in the amphibolitic portion near the contact zone. c) Concentration of titanite crystals in the contact zone between amphibolite and pegmatite. d) Typical mineralogical association of the inner portion of the Tanno pegmatite, characterized by the occurrence of quartz, feldspar, plagioclase, muscovite, garnet, zircon, columbite and beryl. e) Typical amphibole zoning in the inner amphibolitic portion. f) Plagioclase appearance in the amphibolitic portion near the contact zone. g) Contact zone between amphibolite and pegmatite. h) Typical mineralogical association of the inner portion of the Tanno pegmatite.
Amp- amphibole; Phl- phlogopite; Pl- plagioclase; Qz- quartz; Ttn- titanite; Grt- garnet; Zrn- zircon; Brl- beryl; Ms- muscovite; Cl- columbite.

dell'Ambiente, University of Milano-Bicocca. MicroCT slices were then processed with the Avizo Fire (FEI-VSG™) software for 3D-reconstruction and rendering.

RESULTS

Textural analysis

Six samples were used for this study: TT2B.1, representative of the inner amphibolitic portions; TT2B, TT2C, TT2A, located at the contact zone between amphibolite and pegmatite; P3 and TT2D, located respectively in the intermediate and inner portion of the pegmatitic dyke. The inner amphibolite is medium-fine grained and displays disorganized texture, lacking any shape preferred orientation of mineral phases. The mineralogy consists of amphibole, phlogopite, ilmenite and minor fluorapatite, titanite, rutile, Nb-rich rutile and zircon (Fig. 4a). The amphibole has a patchy compositional zoning, as observed in the back-scattered electron images in (Fig. 4e), with the occurrence of two co-existing amphiboles. By means of EPMA analyses, we identified the occurrence of domains with a composition falling in the edenite-pargasite field (Leake et al., 1997), associated to darker domains (Fig. 4e) with a Mg-hornblende composition. Phlogopite occurs as a ubiquitous phase, with more pronounced modal abundance where allanite group minerals are present as well. The amphibolites have a peculiar mineralogy marked by the absence of plagioclase (Fig. 1S), a common phase at greenschist to amphibolite facies conditions in metamorphic mafic rocks. Plagioclase occurs only within a few centimetres from the contact with the pegmatite (Fig. 4b and f) together with titanite, which is commonly absent in the hosting amphibolite where the Ti-bearing phase is ilmenite. Also, fluorapatite appears in the amphibolite only close to the contact.

The pegmatite within 1-2 cm from the contact is fine-grained and presents an anisotropic texture. In this zone, the mineralogical association is composed of quartz, plagioclase, fluorapatite and, to a lesser extent, of K-feldspar, muscovite, pargasite, garnet and biotite (Fig. 4c and g). In the inner pegmatite the grain size become gradually larger reaching, in the core, a maximum of 3-4 cm, while the texture remains very poorly organized (Fig. 4d and h). Garnet is much more frequent and often concentrated in thin layers (Fig. 2S). Plagioclase develops a large grain-size, in particular in the intermediate zone, where centimeter-scale crystals are frequent. It also shows a shape preferred orientation with the elongated axis perpendicular to the contact, developing the typical comb texture of the pegmatite. The inner portions are also characterized by the occurrence of a great variability of REE-bearing accessory mineral phases, in addition to zircon, fluorapatite and columbite-(Fe), also monazite-(Ce), uraninite, xenotime-(Y), betafite and gahnite occur (Fig. 4d).

X-ray micro-computed tomography

The purpose of the X-ray micro-computed tomography (Micro-CT) is the creation of a set of slices that can be overlapped to provide a three-dimensional reconstruction of the sample. The using of the micro-CT reveals, at the millimetre scale, a gradual, diffused and discontinuous contact between the pegmatitic dike and the host amphibolite, characterized by a recurrent and extended interpenetration between the two components, revealing that the spatial interdigitation is very pronounced (Fig. 5). The amphibolites gradually give space to the pegmatitic dyke, developing an intermediate zone between the two components characterized by a visible loosing of the amphibolites shapes, here noticeable as isolated lobes of small dimensions, among which there is the developing of the pegmatitic portion.

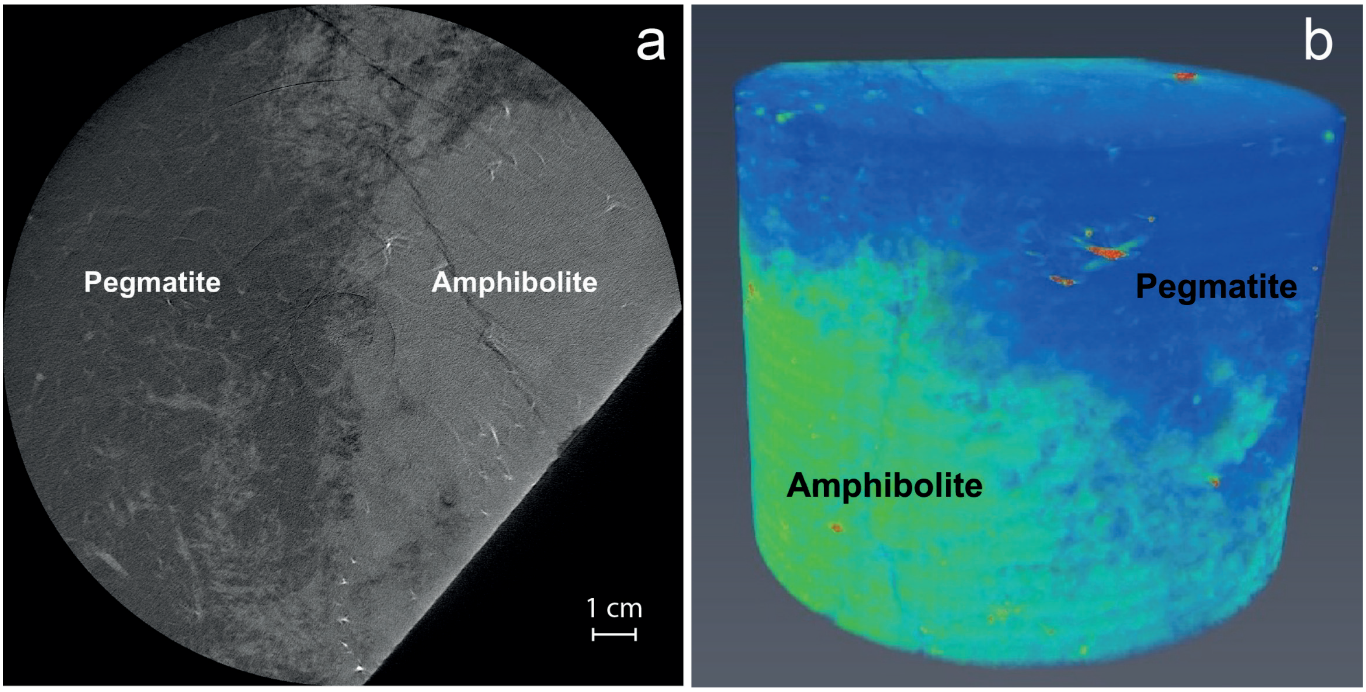

Fig. 5 - a) X-ray computed microtomography showing the contact between hosting amphibolite and the pegmatite dyke. Slice diameters measure 21.37 mm and 17.23 mm. b) 3D - reconstruction of the amphibolte-pegmatite contact. Green colors represent zones with higher density and greater atomic number, blue colors show lower density and smaller atomic number; red spots are denser minerals, such as oxides.

Mineral chemistry

Amphiboles

Amphiboles were normalized on the basis of 23 oxygen and considering Fe^{2+} as Fe total (Table 1S). The classification used for this study (Leake et al., 1997) allowed to distinguish three different amphibole types. Amphibole I and II are in the inner portion of the amphibolite, far from the contact aureole zone. In this area amphiboles have a patchy compositional zoning with variable Mg, Fe, Al and Na content (Fig. 6). Amphibole I is a Mg-hornblende, characterized by Na + K < 0.50 and Ca < 0.50; amphibole II is an edenite-pargasite, i.e. has a Na + K > 0.50 and Ti < 0.50 (Fig. 6a and b). BSE images corroborate two amphiboles generations (Fig. 4e). The brighter grey amphibole is overgrown on the darker grey one. These features are observed also in the TT2A and TT2B amphiboles in the inner amphibolite away from the pegmatite dyke.

Both amphibole I and amphibole II display no significant compositional changes approaching the contact (Fig. 7a and 7b). At the contact with the pegmatite dyke a compositionally homogeneous amphibole, chemically corresponding to a Mg-hornblende (Amphibole III in Fig. 6a), occurs. Amphibole III has an intermediate composition between amphibole I and II, in terms of Na+K content (Fig. 7b), with ($Mg/Mg+Fe^{2+}$) of amphibole II (Fig. 7a).

Micas

Micas belonging to the phlogopite-annite series were normalized on the basis of 11 oxygen atoms and considering Fe^{2+} as Fe total. The mineral chemistry data allow to identify the micas as phlogopites (Table 1S). Phlogopite into the amphibolitic wall rock shows no compositional variations as a function of the distance from the contact with pegmatite (X_{Mg}= Mg/(Mg+Fe) ≈ 0.72).

The muscovite analyses were normalized on the basis of 11 oxygen atoms. The muscovite occurs only into the pegmatitic portions. Muscovite modal abundance increases approaching the dykes core, in which it often presents garnet, zircon, beryl, albite and columbite inclusions.

Plagioclase

The plagioclase analyses were normalized on the basis of 5 cations. Plagioclase occurs along the contact between amphibolite and pegmatite and in the pegmatite as a rock forming mineral. The albite component (Ab = Na/(Na +C a) x 100) of plagioclase in amphibolite increases towards the contact with pegmatite (Fig. 8), shifting from Ab_{45} to Ab_{60}, testifying for chemical exchange reaction between the amphibolite wall rock and the pegmatite dyke (Table 1S). Plagioclase in the pegmatite shows a nearly pure albitic composition at the core of the dyke, whereas Ca-content increases towards the contact reaching 0.6-0.7 (Na/Na+Ca) values (Fig. 8).

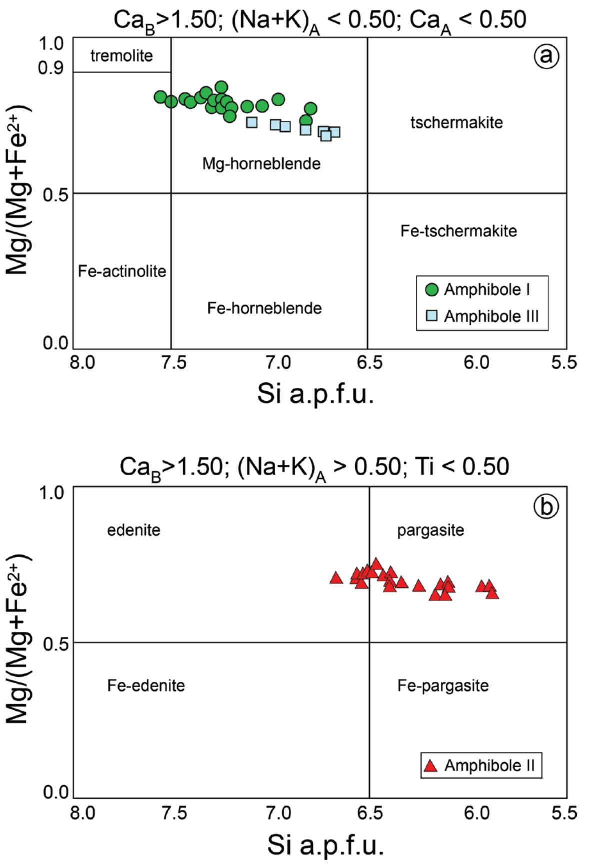

Fig. 6 - Mineralogical composition of amphiboles belonging to the TT2A and TT2B samples, after Leake et al. (1997). a) Mg/(Mg + Fe^{2+}) vs Si (a.p.f.u.) classification diagram for calcic amphibole group. b) Mg/(Mg + Fe^{2+}) vs Si (a.p.f.u.) classification diagram for sodic-calcic amphibole group.

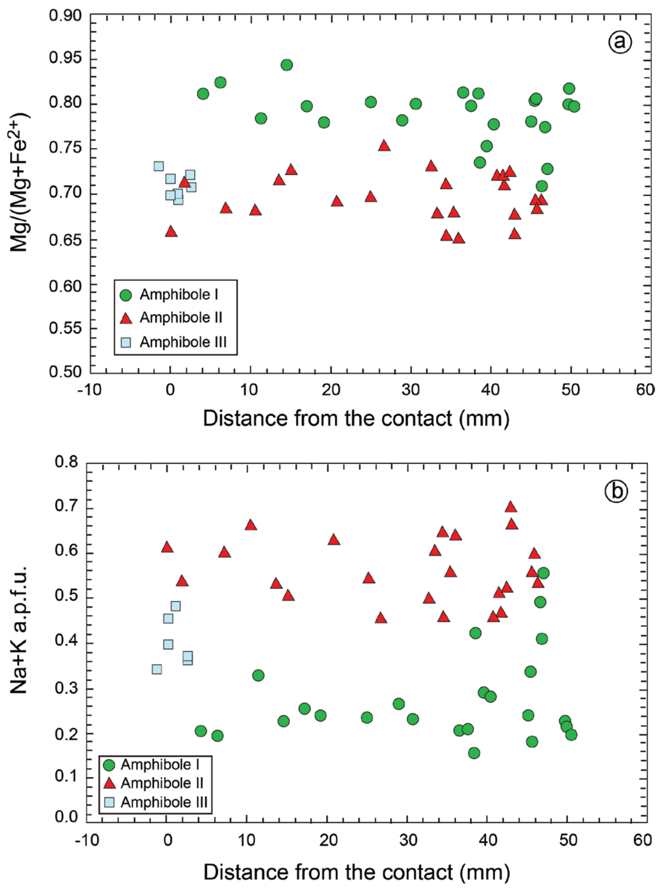

Fig. 7 - a) Variation of Mg/(Mg + Fe^{2+}) in the three amphibole generations as a function of distance from the contact. b) Variation of (Na + K) (a.p.f.u.) in amphiboles as a function of the distance from the contact.

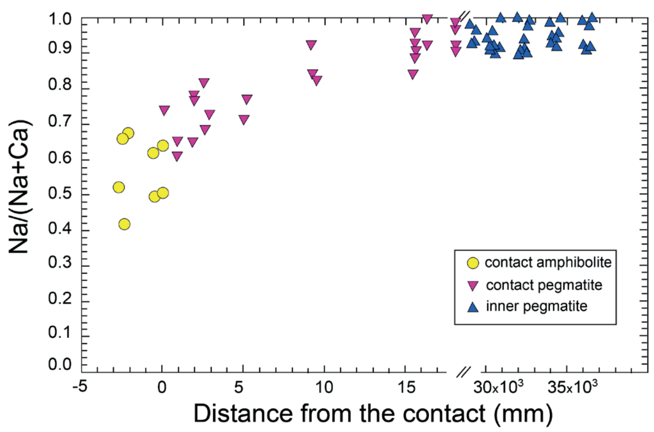

Fig. 8 - Na/(Na + Ca) in plagioclase as a function of the distance from the contact.

K-Feldspar

The K-feldspar analyses were normalized on the basis of 5 cations. The K-feldspar only occurs in the pegmatitic dykes and shows no compositional variations, neither as a function of the distance to the wall rock contact, nor intragranular, within the single feldspar. The medium feldspars composition indicates Or_{94} (Or = K/(Na + K +Ca) x 100) and Ab_6, while the Ca content is negligible (Table 1S).

Garnet

Garnet analyses have been normalized on the basis of 7 cations. They show no compositional variations linked to its position inside the pegmatitic dyke, but there are considerable compositional changes inside the crystals. Garnets are commonly zoned; significant are core to rim Mn variations from 22 wt% in the core down to 15.50 wt% at rim (Table 1S). As displayed by EPMA analyses the decrease of Mn toward the rim corresponds to a Fe^{2+} increase, suggesting that Mn is progressively substituted by Fe^{2+} during garnet growth.

Accessory minerals

The wall rock amphibolite shows a range of accessory minerals, with a prevalence of titaniferous phases as titanite, ilmenite and rutile. Some representative chemical analyses of accessory phases are shown in Table 1. There is also the occurrence, in the amphibolitic contact zone, of fluorapatite, which shows an increase of F percentage approaching the dyke contact. The titanite analyses were normalized on the basis of 5 oxygen atoms, the rutile ones on the basis of 4 oxygen atoms and ilmenite on 3 oxygen atoms.

Gahnite and Th-rich monazite-(Ce) were also analyzed and are characterized by sensible U, Ce, La and HREE contents. Each analyzed pegmatite contains zircon and columbite-(Fe), often zoned, with a Nb-enrichment towards the core of the crystals. The TT2A and TT2D samples have uraninite, xenotime-(Y) and monazite-(Ce) as well. TT2B sample's analysis permitted to recognize a Ti, Nb, Ta oxide belonging to the pyrochlore super-group (Atencio et al., 2010). The gahnite analyses were normalized on the basis 8 oxygen atoms, the columbite ones on the basis of 3 cations and 12 charges, while the betafite ones on the basis of 14 oxygen atoms.

Major, minor and trace elements whole rock analysis

The whole rock analyses (Table 2) show a compositional variability of major elements as a function of the distance from the contact between amphibolite and pegmatite. SiO_2 shows a significant increase towards the pegmatite, and continues to increase from the pegmatite rim to the pegmatite core. The Al_2O_3 content remains instead roughly constant.

Table 1 - Representative chemical compositions (in wt.%) of accessory phases in Tanno amphibolite and pegmatite.

	SiO_2	TiO_2	Al_2O_3	FeO	MnO	MgO	CaO	Na_2O	K_2O	P_2O_5	Nb_2O_5	Ta_2O_5	ZnO	UO_2	F	Total
Apatite																
TT2B	0.05			0.11	0.1		56.5			41.23					3.57	101.55
P5B	0.05			0.03	0.13		55.44			41.01					4.31	100.97
Titanite																
TT2B	30.89	36.67	2.08	0.67	0.06	0.01	28.69		0.02		0.26	0.27	0.02			99.63
P5B	31.17	35.7	2.63	0.59	0.12	0.01	28.73		0.01		0.11	0.06				99.11
TT2B.1	30.63	38.01	1.78	0.67			28.85									99.95
TT2A	30.88	37.47	1.98	0.63			28.7									99.66
Rutile																
TT2B		79.86	0.11	5.55			0.12				8.58	4.17				98.38
Betafite																
TT2B		15.61		0.44	0.19		15.31	1.21	0.12		9.96	31.25	0.06	24.47		98.57
Columbite																
P3		1.04		13.43	6.87	0.12					63.47	14.08	0.06	0.01		99.07
Ilmenite																
P5B		51.95		44.68	2.87	0.61	0.27					0.08				100.38
Gahnite																
P3	0.14		54,00	2.8	0.09	0.13							41.35			98.51

Table 2 - Whole rock major, minor and trace element compositions of Tanno amphibolite and pegmatite (standard deviations in brackets).

wt.%	Inner Pegmatite		Intermediate Pegmatite		Contact Pegmatite		Contact Amphibolite	
SiO_2	75.15	(0.01)	74.95	(0.01)	74.69	(0.01)	42.23	(0.01)
TiO_2	-	-	0.02	-	0.02	(0.01)	1.38	(0.01)
Al_2O_3	15.14	(0.01)	14.81	(0.01)	14.99	(0.01)	14.44	(0.01)
$Fe_2O_{3\,(t)}$	0.18	(0.04)	0.54	(0.04)	0.50	(0.04)	12.33	(0.04)
MnO	0.06	(0.01)	0.10	(0.01)	0.10	(0.01)	0.31	(0.01)
MgO	0.06	(0.01)	0.06	(0.01)	0.06	(0.01)	15.95	(0.01)
CaO	2.56	(0.01)	0.72	(0.01)	0.60	(0.01)	6.45	(0.01)
Na_2O	6.00	(0.01)	4.97	(0.01)	5.10	(0.01)	0.73	(0.01)
K_2O	0.33	(0.01)	3.17	(0.01)	3.49	(0.01)	4.89	(0.01)
P_2O_5	0.11	(0.01)	0.05	(0.01)	0.04	(0.01)	0.03	(0.01)
Cr_2O_3	-	-	-	-	-	-	0.04	(0.002)
L.O.I.	0.40		0.60		0.40		1.21	
Total	100.00		100.00		100.00		100.00	

ppm	Inner Pegmatite		Intermediate Pegmatite		Contact Pegmatite		Contact Amphibolite	
Ba	10.00	(1.00)	4.00	(1.00)	2.00	(1.00)	167.00	(1.00)
Ni	0.40	(0.10)	0.40	(0.10)	0.40	(0.10)	143.00	(0.10)
Sc	-	(1.00)	2.00	(1.00)	2.00	(1.00)	39.00	(1.00)
Be	30.00	(1.00)	11.00	(1.00)	7.00	(1.00)	31.00	(1.00)
Co	0.50	(0.20)	-		0.30	(0.20)	58.10	(0.20)
Cs	2.00	(0.10)	7.30	(0.10)	6.20	(0.10)	172.50	(0.10)
Ga	14.80	(0.50)	18.00	(0.50)	16.80	(0.50)	12.60	(0.50)
Hf	0.50	(0.10)	1.20	(0.10)	0.90	(0.10)	2.40	(0.10)
Nb	4.00	(0.10)	17.50	(0.10)	15.10	(0.10)	4.60	(0.10)
Rb	39.10	(0.10)	299.20	(0.10)	320.10	(0.10)	678.80	(0.10)
Sn	1.00	(1.00)	10.00	(1.00)	11.00	(1.00)	6.00	(1.00)
Sr	226.90	(0.50)	6.70	(0.50)	5.60	(0.50)	14.30	(0.50)
Ta	1.60	(0.10)	2.90	(0.10)	2.10	(0.10)	0.50	(0.10)
Th	1.50	(0.20)	2.20	(0.20)	1.20	(0.20)	0.80	(0.20)
U	18.70	(0.10)	14.60	(0.10)	8.10	(0.10)	1.40	(0.10)
V	-	-	-	-	-	-	201.00	(0.80)
W	-	-	1.30	(0.50)	0.90	(0.50)	2.00	(0.50)
Zr	7.20	(0.10)	23.70	(0.10)	16.90	(0.10)	94.90	(0.10)
Y	1.20	(0.10)	9.50	(0.10)	6.80	(0.10)	32.00	(0.10)
La	4.10	(0.10)	5.60	(0.10)	2.80	(0.10)	13.70	(0.10)

ppm	Inner Pegmatite		Intermediate Pegmatite		Contact Pegmatite		Contact Amphibolite	
Ce	8.20	(0.10)	11.00	(0.10)	5.20	(0.10)	38.30	(0.10)
Pr	0.86	(0.02)	1.30	(0.02)	0.58	(0.02)	5.52	(0.02)
Nd	3.00	(0.30)	4.80	(0.30)	2.00	(0.30)	25.40	(0.30)
Sm	0.86	(0.05)	1.43	(0.05)	0.83	(0.05)	5.60	(0.05)
Eu	0.10	(0.02)	0.09	(0.02)	0.03	(0.02)	1.41	(0.02)
Gd	0.46	(0.02)	1.44	(0.02)	0.80	(0.02)	4.73	(0.02)
Tb	0.06	(0.01)	0.28	(0.01)	0.17	(0.01)	0.73	(0.01)
Dy	0.31	(0.05)	1.77	(0.05)	1.18	(0.05)	5.04	(0.05)
Ho	0.04	(0.02)	0.32	(0.02)	0.20	(0.02)	1.21	(0.02)
Er	0.07	(0.03)	0.83	(0.03)	0.65	(0.03)	4.10	(0.03)
Tm	0.01	(0.01)	0.13	(0.01)	0.09	(0.01)	0.66	(0.01)
Yb	0.09	(0.05)	1.00	(0.05)	0.64	(0.05)	4.85	(0.05)
Lu	-	-	0.15	(0.05)	0.11	(0.05)	0.82	(0.05)
Cu	2.30	(0.10)	1.50	(0.10)	1.00	(0.10)	7.00	(0.10)
Pb	3.40	(0.10)	1.50	(0.10)	1.70	(0.10)	3.30	(0.10)
Zn	6.00	(1.00)	9.00	(1.00)	12.00	(1.00)	73.00	(1.00)
As	0.80	(0.50)	0.80	(0.50)	0.80	(0.50)	1.10	(0.50)
Bi	0.90	(0.10)	0.80	(0.10)	0.80	(0.10)	3.20	(0.10)
Au	0.60	(0.50)	0.80	(0.50)	1.70	(0.50)	2.30	(0.50)
Tl	0.20	(0.10)	-	-	-	-	3.70	(0.10)

FeO and MgO decrease towards the pegmatite, whilst Na_2O describes an opposite trend. K_2O evidences an elevated concentration along the pegmatite contact, while CaO is very abundant into the wall rock. TiO_2 exhibits a higher concentration in the amphibolite. The remaining elements do not show significant variations across the contact.

Trace elements concentration in the analyzed samples are reported in Table 2. The trace elements pattern of the pegmatite, normalized to chondrite (McDonough and Sun, 1995), shows enrichment in LILEs (large-ion lithophile elements) with respect to HFSEs (High Field Strength Elements). With respect to other HFSE, Zr, Nb and Ta, show higher concentrations, as they have been likely partitioned within Fe and Ti oxides (London, 2008), abundant in the pegmatite. REE pattern shows a slight enrichment in LREE with respect to HREE, even though their total tenor remains low (Fig. 9).

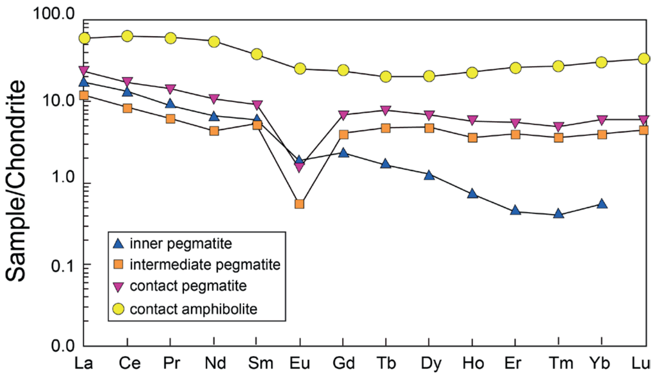

Fig. 9 - Chondrite normalized REE pattern of analyzed amphibolite and pegmatite (McDonough and Sun, 1995).

DISCUSSION AND CONCLUSIONS

Thermal regime

The macro-scale analyses of the Tanno pegmatitic body reveals a series of tabular, sub-planar and parallel dykes which crosscut the amphibolites of the Chiavenna Unit. The pegmatitic melt emplacement took place between 25±0.5 Ma (A. Guastoni, pers. comm). The thermal regime can be assumed to be ca. 550-600°C, the same temperature resulted from a study concerning the emplacement of the close Val Codera pegmatitic field. On the other hand, the amphibolite wall rock had, at the time of the emplacement, a similar temperature, as indicated by the isograds calculated for the Barrovian metamorphism of the Lepontine Dome (Todd and Engi, 1997). Following these data, the ambient temperature of the most amphibolites, at the time of the Tanno pegmatite intrusion, should had been approximately 550°C. A small temperature difference between the two systems had significant consequences on the geometry and metasomatism of the contact between dykes and wall rock, accordingly far to be sharp and with several interpenetrations. The X-ray micro-computed tomography of the contact portion showed, more in detail, what was observed at the outcrop scale, which is a complex geometric interaction between the two bodies, due to their small temperature difference.

Wall rock-dyke interactions

The contact between wall rock and pegmatitic melt caused a chemical disequilibrium in the system, enhanced by the elevate temperature, promoting chemical interactions between the two components, as highlighted by the peculiar distribution gradient for some elements. Whole rock analyses show the variation of some elements concentrations as a function of the distance from the contact, both in terms of major elements and trace elements. The study of the mineralogical phases and their mineral chemistry across the contact provide data in agreement with the X-ray fluorescence whole rock analysis.

One of the most striking features related to the melt-rock interaction is the disappearance of plagioclase in amphibolite far from the contact and its appearance, at about 5 mm from the contact towards the pegmatite.

The amphibolites of the Chiavenna Unit usually display a banded texture, characterized by a compositional layering with interleaved amphibole-rich and plagioclase-rich levels. The amphibolites hosting the Tanno pegmatites are somewhat different, as they are chiefly made of hornblende and accessory minerals and plagioclase is substantially lacking. Plagioclase appears only close, within 5 mm, to the contact and thus we suggest that his growth is strictly related to a melt-rock reaction. Furthermore, the plagioclase composition (Fig. 8) shows an increasing Na-content towards the contact, perfectly comparable to the albitic increase, towards the core, inside the pegmatite.

The plagioclase disappearance away from the contact correspond to other textural and compositional changes inside the amphibolite. Amphiboles away from the contact (Amphibole I and Amphibole II) are characterized by a patchy compositional zoning with compositions ranging from horneblenditic to edenitic terms (Fig. 6). Compositional zoning of amphiboles disappears moving towards the contact, together with the appearance of plagioclase. Within 5 mm from the contact amphiboles (Amphibole III) display an horneblenditic homogeneus composition (Fig. 6), suggesting that the original compositional zoning preserved away from the pegmatite, has been re-homogenized due to thermal effect and melt-rock reaction. Amphibole modal abundance also tends to decrease gradually towards the contact, in favour of a modal increase of phlogopite. Phlogopite shows no particular compositional variations, with the exception of a slight decrease in Ti-content towards the contact.

Concerning the accessory phases, they also show some variations in the contact amphibolite. Fluorapatite appears close to the contact; this is likely due to the elevate phosphorous supply of the pegmatitic melt, together with a greater Ca availability. For the same reason, i.e. Ca availability, titanite substitutes ilmenite as the Ti-bearing phase in the amphibolite.

Inside the pegmatitic dykes the consequences of the interactions between the two components result less evident. From the textural point of view there is a sharp decrease of the grain-size in proximity of the contact, likely due to faster cooling of the pegmatitic melt with respect to the core of the dyke. Concerning the compositional variations, Na content in plagioclase increases towards the core, with a stabilization, at about 2 cm from the contact, at values close to Ab_{95} (Fig. 8 and Table 1S).

Further information on the chemical gradients between amphibolite and pegmatite can be derived by trace element distribution. Sr exhibits a particular trend as a function of the distance from the contact, with higher concentration both in inner amphibolites and in inner pegmatite, as compared with the drastic decrease recorded in proximity of the contact. Also, Ba content varies significantly moving away from the contact, showing a higher concentration nearby the rim, where modal abundance of phlogopite and biotite, main Ba reservoirs, increases. While LREEs show little variations, HREEs vary substantially between the inner and the outer pegmatitic portions. In fact, the HREEs show an increase in proximity of the contact, likely due to the vicinity of amphibolite, where HREE contents are significantly higher with respect to pegmatite. The HREE enriched composition of the pegmatite close to the contact could be explained by the occurrence of numerous titanite crystal, that are lacking in the pegmatite core. Titanite could be a HREEs reservoir (Mulrooney and Rivers, 2005) and its concentration along the pegmatite external contact could explain the high HREE contents displayed by whole rock data (Fig. 9 and Table 2).

As regards to the remaining REEs, as previously mentioned, they do not show particular variations inside the pegmatite; nonetheless a significant increase in the contact area is observable. This can be attributed to the high concentration, inside the amphibolite, of allanite group minerals. The melt-rock interaction caused the destabilization of this accessory mineral, which, indeed, was not observed in proximity of the contact. The mobilized REEs affected the pegmatitic contact portion, recorded by variations in the REEs ditribution.

The occurrence of gahnite, a Zn-bearing spinel, plays an important role for the understanding of the pegmatitic melt nature. Its presence indicates that this pegmatite belongs to the LCT (Lithium, Cesium, Tantalum) petrogenetic family (Černý and Ercit, 2005), characterized by the presence of significant amounts of Li, Ce and Ta. In addition, the distribution of Zn and Mn compared to Fe and Mg indicates relatively high degree of fractionation, which allows to classify this pegmatite as belonging to the rare-element class.

Profiting of mineralogical distribution across the contact, of mineral chemistry variations and of distribution of major and trace elements across the contact, we suggest the following reaction, responsible of all changes we observed at different scales:

Amphibole I + Amphibole II + Ilmenite + Pegmatitic melt
→ Amphibole III + Plagioclase + Phlogopite + Titanite
+ Apatite

This reaction describes the interaction between the melt and the wall rock. Melt-rock reaction caused the destabilization of two inner amphiboles (edenite and Mg-horneblende, Fig. 10), which gave space to a third amphibole, characterized by an intermediate horneblenditic composition. The great K supply from the melt allowed the concentration of a great phlogopite modal abundance, while plagioclase, during the crystallization, received a greater amount of Ca (obtained from the pegmatitic melt supply and from the primary Ca-amphibole destabilization) that modified the composition towards a greater anorthitic composition. This is in contrast with the plagioclase belonging to the pegmatite, which is strongly albitic in composition, reaching values close to Ab_{95}. The interaction also caused the break-down of ilmenite which, as observed in BSE images and petrographic observations, is absent in proximity of the contact, giving space to the titanite, which increases its modal abundance due to the Ca supply from the amphibolite.

Furthermore, the appearance, inside the amphibolite and in proximity of the contact, of fluorapatite, can be attributed to the high P supply from the pegmatitic melt combined with the increased Ca availability.

Despite the different interactions described, the amphibolitic reaction area in which the reaction occurs extends for 5 mm starting from the contact. This is simply noticeable considering that the pegmatitic melt was extremely depleted in fluids at the time of the emplacement into the wall rock.

Conclusions

In this study, we examined the interactions between the Tanno pegmatitic field and the hosting amphibolites of the Chiavenna ophiolitic unit. Textural, mineralogical and geochemical analyses allowed to individuate the occurrence of melt-rock interactions at the millimetre scale along intrusive contacts. On the basis of the whole rock geochemical data and mineral chemistry, it was possible to trace the petrogenetic features of the pegmatitic bodies. The mineralogical association of the pegmatites is made of quartz, Na-rich plagioclase, K-feldspar, garnet (almandine-spessartine), muscovite, biotite and a wide range of accessory minerals, that allow to obtain information on the pegmatite type and evolution. The presence of gahnite was fundamental in order to study the melt differentiation degree, which was proved to be evolved. The pegmatitic dykes intruded an amphibolitic wall rock, whose mineralogical association is made by amphibole, phlogopite, titanite, rutile, ilmenite, allanite group minerals and zircon.

Despite at the outcrop scale the intrusive contact between the pegmatitic dyke and the amphibolitic wall rock is sharp, a detailed sampling across the contact and related analyses allowed to identify both for amphibolite and pegmatite the occurrence of compositional variability dependent on the distance to the contact. SiO_2 and Na_2O increase from the amphibolites towards the pegmatite, while CaO, FeO and MgO show an opposite trend. This variability is clearly followed

Amphibole I + Amphibole II + Ilmenite + Pegmatitic melt (F, P, K) →

Amphibole III + Plagioclase + phlogopite + Titanite + Apatite

Inner pegmatite	Contact pegmatite	Contact amphibolite	Inner amphibolite
plagioclase, quartz, muscovite, K-feldspar, garnet, biotite (zircon, columbite, uraninite, gahnite, xenotime, monazite, apatite)	plagioclase, quartz, biotite, pargasite	phlogopite, plagioclase, titanite, apatite, Mg-horneblende II	Mg-horneblende I, edenite, phlogopite, ilmenite (titanite, rutile, allanite)

→ MgO, K_2O, CaO

← SiO_2, Al_2O_3, Na_2O

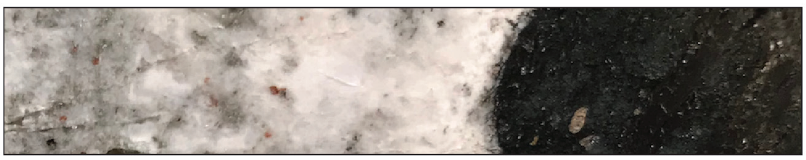

Fig. 10 - Variable mineralogical and whole rock composition, integrated with X-ray fluorescence data from an inner portion of the same amphibolite (Liati et al., 2003), as a function of the distance from the contact between amphibolite and pegmatite. A picture of the contact zone is shown as well.

by mineral chemistry variations, mainly observable in phases such as plagioclase and amphibole. The amphibolite equilibrium mineral assemblage does not contain plagioclase, which anyhow appears in proximity of the contact. From the plagioclase starting point inside the amphibolite towards the pegmatite core, it describes a gradual increase of the albitic content.

On the basis of these observations, it was possible to individuate, in proximity of the contact, the developing of a limited reaction area characterized by the appearance of plagioclase, titanite, phlogopite and fluorapatite. This mineralogical association is the result of the interaction between the pegmatitic melt and the amphibolite, as a result of a significant compositional gradient between the two portions. The developing of an extended chemical interaction between amphibolite and pegmatite was possible due to the small temperature difference at the time of the intrusion. This permitted the development of a marked micro-scale interdigitation in the contact zone, which enhanced the chemical relationships between the two portions.

This study opens new scenarios aimed at the comprehension of the mechanism and origin of the Tanno pegmatitic bodies and their relationships with the wall-rocks.

ACKNOWLEDGEMENTS

We greatly appreciated suggestions and comments by L. Secco and an anonymous reviewer who revised the first version of the manuscript: they helped us to significantly improve the paper quality. We wish to thank also A. Montanini for the editorial handling of the paper. Andrea Risplendente is greatly thanked for the careful electron-microprobe analyses. This research has been supported by the Italian Ministry of Education, University and Research (MIUR) through the grant [PRIN-2015C5LN35] “Melt–rock reaction and melt migration in the MORB mantle through combined natural and experimental studies”.

Supplementary data to this article are available online at https://doi.org/10.4454/ofioliti.v45i1.530

REFERENCES

Atencio A., Andrade M.B., Christy A.G., Gieré R. and Kartashov P.M., 2010. The pyrochlore supergroup of minerals: nomenclature. Can. Miner., 48: 673-698.

Burri T., Berger A. and Engi M., 2005. Tertiary migmatites in the Central Alps: Regional distribution, field relations, conditions of formation and tectonic implications. Schweiz. Miner. Petrogr. Mitt., 83: 215-235.

Černý P. and Ercit T.S., 2005 The classification of granitic pegmatites revisited. Can. Miner., 43: 2005-2026.

Galli A., Le Bayon B., Schmidt M.W., Burg J.P., Reusser E., Sergeev S.A. and Larionov A., 2012. U-Pd zircon dating of the Gruf Complex: disclosing the late Varisican Granulitic lower crust of Europe stranded in the Central Alps. Contrib. Miner. Petrol., 163: 353-378.

Guastoni A., Pennacchioni G., Pozzi G., Fioretti A.M. and Walter J.M., 2014. Tertiary pegmatites dikes of the Central Alps. Can. Miner., 52: 191-219.

Huber R.K. and Marquer D., 1998 The tectonometamorphic history of the peridotitic Chiavenna unit from Mesozoic to Tertiary tectonics: a restoration controlled by melt polarity indicators (Eastern Swiss Alps). Tectonophysics, 296: 205-223.

Leake B.E., Woolley A.R., Birch W.D., Gilbert M.C., Grice J.D., Hawthorne F.C., Kato A., Kisch H.J., Krivovichev V.G., Linthout K., Lird J. and Mandarino J., 1997. Nomenclature of amphiboles: report of the subcommittee on amphiboles of the International Association Commission on New Minerals and Mineral Names. Miner. Mag., 61: 295-321.

Liati A., Gebauer D. and Fanning M., 2000. U-Pb SHRIMP dating of zircon from the Novate granite (Bergell, Central Alps): evidence for Oligocene-Miocene magmatism, Jurassic/Cretaceous continental rifting and opening of the Valais trough. Schweiz. Miner. Petrogr. Mitt., 80: 305-316.

Liati A., Gebauer D. and Fanning M., 2003. The youngest basic oceanic magmatism in the Alps (Late Cretaceous; Chiavenna unit, Central Alps): geochronological constraints and geodynamic significance. Contrib. Miner. Petrol., 146: 144-158.

London D., 2008. Pegmatites. Can. Miner. Spec. Publ., 10, 347 pp.

McDonough W.F and Sun S., 1995 The composition of the Earth. Chem. Geol., 120: 223-253.

Mulrooney D. and Rivers T., 2005. Redistribution of the rare-earth elements among coexisting minerals in metamafic rocks across the epidote-out isograd: an example from the St. Anthony Complex, northern Newfoundland, Canada. Can. Miner., 43: 263-294.

Nicollet C., Bosse V., Spalla M.I. and Schiavi F., 2018. Eocene ultra-high temperature (UHT) metamorphism in the Gruf Complex (Central Alps): constraints by LA-ICPMS zircon and monazite dating in petrographic context. J. Geol. Soc. London, 175: 774-787.

Oschidari H. and Zieger U.R.F., 1992. Vergleichende Sm-Nd und Rb-Sr Unterschungen and Bergeller Gerollen aus der Gonfolite Lombarda (“Sudalpine Molasse”) und an Bergeller und Novate Granitoiden des Ursprungsgebietes. Ecl. Geol. Helv., 85: 375-384.

Ring U., 1992 The Alpine geodynamic evolution of Penninic nappes in the eastern Central Alps: geothermobarometric and kinematic data. J. Metam. Geol., 10: 33-53.

Rosenberg C.L., Berger A. and Schmid S.M., 1995. Observations from the floor of a granitoid pluton: inferences on the driving force of final emplacement. Geology, 23 (5): 443-446.

Rubatto D., Hermann J., Berger A. and Engi M., 2009. Protracted fluid-induced melting during Barrovian metamorphism in the Central Alps. Contrib. Miner. Petrol., 158: 703-722.

Schmid S.M., Aebli H.R., Heller F. and Zing A., 1989. The role of the Periadriatic Line in the tectonic evolution of the Alps. In: M.P. Coward, D. Dietrich, R.G. Park (Eds.), Alpine tectonics. Geol. Soc. London, p. 153-171.

Schmid S.M., Rück P. and Schreurs G., 1990. The significance of the Schams nappes for the reconstruction of the paleotectonic and orogenic evolution of the Penninic zone along the NFP-20 East traverse (Grisons, eastern Switzerland). Mém. Soc. Géol. Fr., 156: 263-287.

Steinmann M. and Stille P., 1999. Geochemical evidence for the nature of the crust beneath the eastern North Penninic basin of the Mesozoic Tethys Ocean. Intern. J. Earth Sci., 87: 633-643.

Stucki A., Rubatto D. and Trommsdorff V., 2003. Mesozoic ophiolite relics in the Southern Steep Belt of the Central Alps. Schweiz. Miner. Petrogr. Mitt., 83: 285-299.

Talerico C., 2001. Petrological and chemical investigation of a metamorphosed oceanic crust-mantle section (Chiavenna, Bergell Alps). Tesi dott., ETH Zurich, 153 pp.

Todd C.S. and Engi M., 1997. Metamorphic field gradients in the Central Alps. J. Metam. Geol., 15: 513-530.

Trommsdorf V., 1966. Progressive metamorphose kieseliger karbonatgesteine in den zentralalpen zwischen Bernina und Simplon. Schweiz. Miner. Petrogr. Mitt., 46: 431-460.

von Blackenburg F., 1992. Combined high-precision chronometry and geochemical tracing using accessory minerals: applied to the Central-Alpine Bergell intrusion (central Europe). Chem. Geol., 100: 19-40.

von Blanckenburg F., Fruh-Green G., Diethelm K.H and Stille P., 1992. Nd-, Sr, O-isotopic and chemical evidence for a two stage contamination history of mantle magma in the Central Alpine Bergell intrusion. Contrib. Miner. Petrol., 110: 33-45.

Received, December 5, 2019
Accepted, Dcember 30, 2019
First published online, January 3, 2020